ISTITUTO NAZIONALE DI FISICA NUCLEARE

Sezione di Genova

INFN/AE-80/3
14 Luglio 1980

E. Di Salvo and G. A. Viano: SURFACE WAVES IN PION-PROTON ELASTIC SCATTERING.

Servizio Documentazione
dei Laboratori Nazionali di Frascati

Istituto Nazionale di Fisica Nucleare
Sezione di Genova

INFN/AE-80/3
14 Luglio 1980

E. Di Salvo and G.A. Viano: SURFACE WAVES IN PION-PROTON ELASTIC SCATTERING.

ABSTRACT. - We present a phenomenological analysis of the pion-proton elastic scattering, at intermediate energies, based on the theory of surface waves. These are excited at the edge of the interaction region and propagate along it, being damped in the direction of propagation. Since at the energies, where we are working, the black-body limit is not yet reached, the surface waves can also take one or more shortcuts inside the interaction region. This fact explains the enhancement of the cross-section at backwards. Many points of the theory can be phenomenologically checked, and the interaction radius, in the pion-proton elastic collision, can be numerically derived.

RIASSUNTO. - Presentiamo un'analisi fenomenologica della collisione elastica pione-protone, ad energie intermedie, basata sulla teoria delle onde superficiali. Queste ultime sono eccitate al bordo della regione d'interazione e si propagano attorno ad essa, attenuandosi nella direzione di propagazione. Alle energie a cui lavoriamo, possiamo assumere che la regione d'interazione non sia totalmente assorbente ; quindi alcune onde superficiali possono penetrare all'interno e percorrere delle "scorciatoie". Ciò permette di spiegare l'innalzamento della sezione d'urto a grandi angoli. Molti punti della teoria possono essere verificati fenomenologicamente. Inoltre si può dedurre numericamente il raggio d'interazione nell'urto elastico pione-protone.

1. - INTRODUCTION.

We consider the elastic scattering of positive pions from an unpolarized proton target in the momentum range 3-7 GeV/c. Following Schrempp[1], we assume that the pion-proton collision in the centre of mass system (c.m.s.) may be reduced to the scattering of a plane wave from a body, which has the shape and the dimensions of the interaction region, identifying the wave number k with the c.m.s. momentum of the colliding particles. We make the hypothesis that the interaction region is a sphere of radius R, centered in the centre of mass.

In the momentum range considered, the small wavelength approximation can be applied; moreover we assume that there is a strong absorption at small impact parameters, but not at large ones. Therefore one can associate with the l-th partial wave an impact parameter $b_l = (l+1/2)/k$ and roughly say that the partial waves with $b_l < R$ are absorbed. More precisely the so called "localization principle" leads to a subdivision of the partial wave series into three domains[2]:

(i) $0 \leqslant l \lesssim l_- = \beta - c\beta^{1/3}$; (ii) $l_- \lesssim l \lesssim l_+ = \beta + c\beta^{1/3}$; (iii) $l_+ \lesssim l$

where $\beta = kR$ and c is a quantity of order unity. Partial waves in the domain (i) are absorbed; those in the domain (iii) are damped by the centrifugal barrier and give a negligible contribution. Finally the waves, belonging to the domain (ii), correspond to incident particles passing close to edge of the target and give rise to surface waves, which propagate along the surface of the body.

The scattering process that we analyze can be described using a complex valued potential such that the real part has a sharp edge and the imaginary part has a radius smaller than the real one. In other words there is a transparent shell at the periphery of the interaction region. This shell disappears towards larger energies, when the "black-body" limit is reached[1]. Therefore the grazing rays may describe simply an arc of geodesic around the body or also take one or more shortcuts before emerging tangentially at the surface. The process is quite involved and it is convenient to use the ray tracing technique, which has been originally introduced in optics. Then we shall speak of a complex valued "refraction index" instead of a potential, and we shall use the concepts and methods of geometrical theory of diffraction in the sense of Keller[3]. Indeed the wave function of the π^+-p system satisfies the stationary Klein-Gordon equation[1], which is formally identical to the stationary wave equation, so that, in the limit of large k, the methods of Keller's theory can be extended to our case. Therefore, hereafter, we shall use words typical of optics, like diffraction, reflection, refraction and so on, which shall refer, in this case, to particle trajectories rather than to light rays.

Up to now, as far as we know, only the case of high frequency scattering by a transparent sphere[2] (or a wholly opaque sphere[4, 5]) has been considered in detail. The mathematical methods in use are so involved that it appears hopeless, at the moment, to extend these procedures to the realistic case of a "refraction index" strongly absorbing at the centre and with a transparent shell at the periphery. We prefer to follow a more practical attitude, which consists in proposing suitable conjectures to be supported by the phenomenological analysis. Our main conjecture is the following one: we suppose that, while the waves in the domain (i) are absorbed by the opaque core of the target, the waves in the domain (ii) give rise, precisely, to the same phenomena as in the case of a wholly transparent sphere. This conjecture is theoretically reasonable in virtue of the "localization principle" which we have illustrated above. Indeed, thanks to this principle, we can assume that the phenomena which occur at the periphery (i. e. in the transparent shell), are essentially independent of the inner structure of the refraction index.

The paper is organized as follows: in Section 2 we sketch an outline of the theory; Section 3 is devoted to the phenomenological analysis.

2. - OUTLINE OF THE THEORY.

The π^+-p system is described by a wave function satisfying the stationary Klein-Gordon equation[1]:

$$(\nabla^2 + N^2 k^2)\psi = 0 , \qquad r \leq R , \tag{1a}$$

$$(\nabla^2 + k^2)\psi = 0 , \qquad r > R , \tag{1b}$$

where k is the wave number in the c. m. s. and N is the "refraction index". Here we neglect the effects of the spin of the proton. This approximation is acceptable since the target is unpolarized. Moreover we shall verify phenomenologically that the spin-flip amplitude is negligible with respect to the non-spin-flip one.

Let us observe that the equation (1) is formally identical to the wave equation describing a monochromatic beam of light hitting an obstacle. Since $\beta = kR \gg 1$, we can use the same approximation methods as in the optics of the short wavelengths. Therefore translating the methods and terminology of geometrical diffraction theory into the domain of particle dynamics, we can distinguish the following phenomena:

a) reflection at the surface of the sphere;

b) refraction;

c) diffraction of grazing rays; these describe an arc of geodesic around the obstacle and may also shed into limiting refracted rays.

Now the refracted rays cannot cross the opaque core. However we assume that the transparent shell is large enough to allow the critically refracted rays to cross it without being absorbed. Therefore, in evaluating the scattering amplitude we have to take into account the direct reflection, the diffraction and the critical refraction. Moreover we must distinguish between the rays which describe an arc of geodesic around the target and shall be called "surface rays", and those which, being critically refracted, give only a geometrical contribution. In order to be more precise on this point, let us consider a ray which is critically refracted at the point of incidence and takes a shortcut: it may undergo a second critical refraction and emerge in the direction $\vartheta = \vartheta_t$, where ϑ_t is the amplitude of the arc corresponding to the shortcut; or alternatively, it may be internally reflected $1, 2, \ldots, p-1$ times and emerge, after a final critical refraction, in the directions $\vartheta = 2\vartheta_t$, $\vartheta = 3\vartheta_t$, $\ldots$, $\vartheta = p\vartheta_t$, without describing any arc of geodesic. For the moment we do not consider this type of geometrical contribution. Therefore we treat only the reflected and diffracted rays; then the scattering amplitude $f(\beta, \vartheta)$ is given by:

$$f(\beta, \vartheta) = f_r(\beta, \vartheta) + f_d(\beta, \vartheta) , \tag{2}$$

where $f_r(\beta, \vartheta)$ and $f_d(\beta, \vartheta)$ denote respectively the reflection and the diffraction amplitudes. Here, following Nussenzveig[2], we use dimensionless scattering amplitudes; therefore, in order to evaluate the differential cross-sections, we must multiply the modulus squared of f by the factor R^2.

As far as reflection is concerned, we assume that the reflected wave (and therefore the reflection amplitude) depends only on the properties of the obstacle at the point of reflection and on the angle of incidence. As a consequence, we can use the same formula that was found for a wholly transparent sphere[2]:

$$f_r(\beta, \vartheta) = -\frac{1}{2} \frac{\sqrt{N^2 - \cos^2\frac{\vartheta}{2}} - \sin\frac{\vartheta}{2}}{\sqrt{N^2 - \cos^2\frac{\vartheta}{2}} + \sin\frac{\vartheta}{2}} e^{-2i\beta\sin\frac{\vartheta}{2}} \left[1 + O(\beta^{-1})\right] \tag{3}$$

where N is the (real) refraction index in the transparent shell. This formula fails when $\vartheta \lesssim \beta^{-1/3}$, i.e. in a region including the diffractive peak, where reflection at the critical angle occurs; this particular situation will be examined later on. Finally, formula (3) is strictly valid if we assume a sharp edge at the surface of the sphere. In the next Section we shall see how this formula can be modified under more general conditions.

Now let us consider the term $f_d(\beta, \vartheta)$. This has to be further decomposed into different contributions, i.e.

$$f_d(\beta, \vartheta) = f_d^{(o)}(\beta, \vartheta) + \sum_{p \geq 1} f_d^{(p)}(\beta, \vartheta) \tag{4}$$

where $f_d^{(o)}(\beta, \vartheta)$ refers to the surface waves which travel only on the surface, while $f_d^{(p)}(\beta, \vartheta)$, for $p \geq 1$, takes into account the contribution of those rays which have limiting refraction and take p shortcuts.

To evaluate each term of the sum (4), we give a detailed description of the ray tracing of the grazing rays which emerge in a direction $\vartheta (0 \leq \vartheta \leq \pi)$, after taking 0, 1, 2, ..., p shortcuts inside the transparent shell of the sphere. In particular let us consider, for each value of p, the ray tracing for the surface rays, in a way similar to Chen[6] and Nussenzveig[2]. When $p = 0$, a grazing ray describes an arc of amplitude:

$$\zeta^{+}_{0,m} = \vartheta + 2m\pi , \qquad m = 0, 1, 2, \ldots \tag{5a}$$

or

$$\zeta^{-}_{0,m} = 2\pi - \vartheta + 2m\pi , \qquad m = 0, 1, 2, \ldots \tag{5b}$$

where $\zeta^{+}_{0,m}$ is the arc described by the counterclockwise travelling surface wave, while $\zeta^{-}_{0,m}$ is the arc described by the clockwise travelling one (see Fig. 1). When p = 1, the grazing ray may

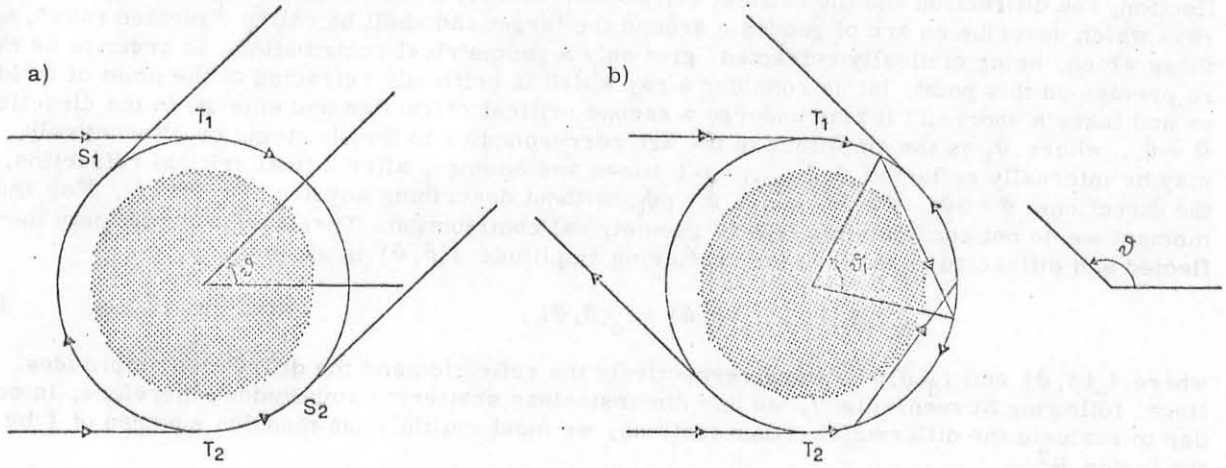

FIG. 1 - Diffracted rays in the direction ϑ. a) p = 0; b) p = 1.

undergo a critical refraction, take a shortcut and reemerge at the critical angle, describing an arc of amplitude:

$$\zeta^{\pm}_{1,m} = \zeta^{\pm}_{1} + 2m\pi \,, \qquad m = 0, 1, 2, \ldots\ldots \tag{6a}$$

where

$$\zeta^{\pm}_{1} = \pm\vartheta - \vartheta_t \pmod{2\pi} \,, \qquad (0 < \zeta^{\pm}_{1} \leq 2\pi) \,. \tag{6b}$$

However, the grazing ray may also describe an arc of amplitude φ $(0 \leq \varphi \leq \zeta^{\pm}_{1,m})$, then take a shortcut and lastly describe an arc of amplitude $\zeta^{\pm}_{1,m} - \varphi$. We have a different ray for any value of φ, so that we must take all these infinite possibilities into account.

For p = 2 the surface rays take two shortcuts, so that the arcs of geodesics have, in all, an amplitude:

$$\zeta^{\pm}_{2,m} = \zeta^{\pm}_{2} + 2m\pi \,, \qquad m = 0, 1, 2, \ldots\ldots \tag{7a}$$

where

$$\zeta^{\pm}_{2} = \pm\vartheta - 2\vartheta_t \pmod{2\pi} \,, \qquad (0 < \zeta^{\pm}_{2} \leq 2\pi) \,. \tag{7b}$$

In this case we must consider two different kinds of rays:

i) the rays that describe an arc φ at the surface $(0 \leq \varphi \leq \zeta^{\pm}_{2,m})$, then take two shortcuts consecutively and, lastly, describe an arc of amplitude $\zeta^{\pm}_{2,m} - \varphi$. We have a different ray for any value of φ.

ii) the rays that describe an arc φ_1 $(0 \leq \varphi_1 \leq \zeta^{\pm}_{2,m})$, then take a shortcut, reemerge describing an arc φ_2 $(0 < \varphi_2 \leq \zeta^{\pm}_{2,m} - \varphi_1)$ and, after another shortcut, describe an arc of amplitude $\zeta^{\pm}_{2,m} - \varphi_1 - \varphi_2$; we have a different ray for each value of φ_1 and φ_2.

Consequently the type (i) rays can be traced in a simply infinite number of ways, while the type (ii) can take place in a doubly infinite number of ways.

For a general value of p, a ray, before emerging in a direction ϑ, has to describe arcs of amplitudes φ_j such that:

$$\sum_j \varphi_j = \zeta^{\pm}_{p,m} = \zeta^{\pm}_p + 2m\pi , \qquad m = 0, 1, 2, \ldots . \tag{8a}$$

where

$$\zeta^{\pm}_p = \pm \vartheta - p\vartheta_t \pmod{2\pi} \qquad (0 < \zeta^{\pm}_p \leq 2\pi) . \tag{8b}$$

We must consider p different kinds of rays, according as they have $0, 1, \ldots, p-1$ internal reflections. In this connection it is useful to distinguish between type (i) and type (ii) vertices: we denominate type (i) vertices those at which an internal reflection takes place, type (ii) vertices those at which two critical refractions occur (see Fig. 2). In the simplest case the ray describes an arc φ, then it has p-1 internal reflections (i.e. (p-1) type (i) vertices) and lastly describes an arc $\zeta^{\pm}_{p,m} - \varphi$. Another class of rays can be obtained by substituting one type (i) by one type (ii) vertex. Similarly, all the possible classes of rays are obtained by substituting $2, 3, \ldots$ type (i) vertices by $2, 3, \ldots$ type (ii) vertices.

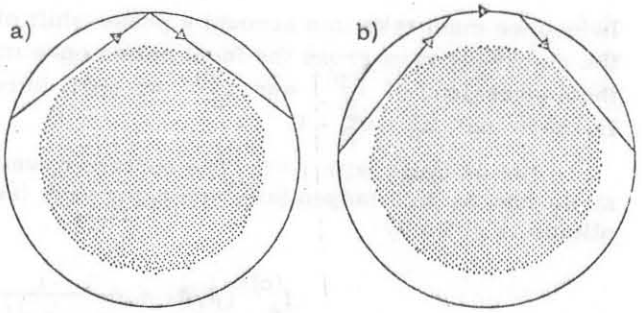

FIG. 2 - Two types of vertices. a) One internal reflection (type (i) vertex); b) Two critical refractions (type (ii) vertex).

In order to compute the contributions of the rays to the scattering amplitude, we must distinguish among the different "interactions" of the ray with the surface. More precisely, we may regard as an "interaction-vertex" any point at which diffraction, critical refraction or internal reflection takes place. Consequently, we may define a proper "coupling constant" for any type of interaction. They are:

a) the diffraction coefficient D_n;

b) D_{12} and D_{21} for the rays which have a critical refraction entering into, or emerging from the sphere;

c) R_{22} for the internal reflection.

Note that we assume these coefficients to be dimensionless. Moreover, the line joining two "vertices" can be regarded as a "propagator". We must distinguish between two cases, which are the following ones:

a) the "propagator" for a shortcut is given by

$$e^{ik\{2\sqrt{N^2-1}\,R\}} = e^{2i\beta\sqrt{N^2-1}} \tag{9}$$

where $2\sqrt{N^2-1}\,R$ is the optical path length of the shortcut;

b) for a surface ray describing an arc of amplitude φ_j the "propagator" takes the form

$$e^{i\lambda_n \varphi_j} \tag{10}$$

where $\lambda_n = \beta + i\alpha_n$, α_n being the decay exponents of the surface waves.

Furthermore, due to the geometry of the obstacle, the diffracted rays form an axial caustic, which is the straight line parallel to the incident beam and passing through the centre of the sphere. On the caustic the ray approximation is no longer valid; however we take into account

the focusing effect with the factor $(\sin\vartheta)^{-1/2}$, provided that we are sufficiently far from the caustic itself.

Next we do two simplifying assumptions :

a) we do not take into account the rays for which $m \geq 1$;

b) we consider only that surface wave for which $\mathrm{Re}\,\alpha_n$ is the lowest one, i. e. $n = 1$. This latter approximation does not hold in the transition regions, which will be defined subsequently.

Finally it is convenient to split $f_d^{(p)}(\beta,\vartheta)$ into the contributions of the counterclockwise and clockwise rays, i. e.

$$f_d^{(p)}(\beta,\vartheta) = f_d^{(p)+}(\beta,\vartheta) + f_d^{(p)-}(\beta,\vartheta) \quad . \tag{11}$$

Indeed we must take into account a phase-shift of $-\pi/2$ between $f_d^{(p)-}(\beta,\vartheta)$ and $f_d^{(p)+}(\beta,\vartheta)$, since the clockwise rays cross the focal points once more than the counterclockwise ones. Therefore in the expressions of $f_d^{(p)+}$ and $f_d^{(p)-}$ we shall introduce two phase factors $i^{n_p^+}$ and $i^{n_p^-}$ respectively, such that $n_p^- = n_p^+ - 1$.

Let us begin with $p = 0$. The surface waves are excited at T_1 and T_2, and are reconverted at S_1 and S_2 into tangentially emerging rays (see Fig. 1). The contribution to the scattering amplitude is given by :

$$f_d^{(o)+}(\beta,\vartheta) = \frac{-i}{(\sin\vartheta)^{1/2}}\, D_1\, e^{i\lambda_1\vartheta}\, D_1 \quad , \tag{12a}$$

$$f_d^{(o)-}(\beta,\vartheta) = \frac{-1}{(\sin\vartheta)^{1/2}}\, D_1\, e^{i\lambda_1(2\pi-\vartheta)}\, D_1 \quad . \tag{12b}$$

Next let us consider the contribution for $p = 1$; we have :

$$f_d^{(1)+}(\beta,\vartheta) = \frac{i^{n_1^+}}{(\sin\vartheta)^{1/2}}\, D_1 \left\{ \int_0^{\zeta_1^+} e^{i\lambda_1\varphi}\, D_{12}\, e^{2i\beta\sqrt{N^2-1}}\, D_{21}\, e^{i\lambda_1(\zeta_1^+-\varphi)}\, d\varphi \right\} D_1 = \tag{13a}$$

$$= \frac{i^{n_1^+}}{(\sin\vartheta)^{1/2}}\, D_1^2 D_{12} D_{21}\, e^{2i\beta\sqrt{N^2-1}}\, e^{i\lambda_1\zeta_1^+}\, \zeta_1^+ \quad .$$

We have carried out the integration over φ in order to consider all the possible ways in which a ray with $p = 1$ can be traced.

Similarly we get :

$$f_d^{(1)-}(\beta,\vartheta) = \frac{i^{n_1^-}}{(\sin\vartheta)^{1/2}}\, D_1^2 D_{12} D_{21}\, e^{2i\beta\sqrt{N^2-1}}\, e^{i\lambda_1\zeta_1^-}\, \zeta_1^- \quad . \tag{13b}$$

Now we can generalize this procedure to any value of p. Besides the focusing factor, we have the common factor $D_1^2 D_{12} D_{21}$, due to initial and final diffraction and critical refraction. Moreover we have to consider p "propagators" of type (9), i. e. $e^{2ip\beta\sqrt{N^2-1}}$, and a number of "propagators" of type (10), i. e.

$$\prod_j e^{i\lambda_1\varphi_j} = e^{i\lambda_1\sum_j\varphi_j} = e^{i\lambda_1\zeta_p^{\pm}} \quad . \tag{14}$$

Lastly we must take into account all the possible ways in which the intermediate interactions take place. In the case of (p-1) internal reflections (i. e. when all the vertices are of type (i)) we have a contribution of

$$(R_{22})^{(p-1)} \int_0^{\zeta_p^{\pm}} d\varphi = (R_{22})^{(p-1)} \zeta_p^{\pm} . \tag{15}$$

Next we can substitute one type (i) by one type (ii) vertex in (p-1) different ways ; the contribution is :

$$(p-1)(R_{22})^{(p-2)} D_{12}D_{21} \int_0^{\zeta_p^{\pm}} d\varphi_1 \int_0^{\zeta_p^{\pm} - \varphi_1} d\varphi_2 = (p-1)(R_{22})^{(p-2)} D_{12}D_{21} \frac{(\zeta_p^{\pm})^2}{2!} . \tag{16}$$

The substitution ot two type (i) by two type (ii) vertices can be done in $\frac{(p-1)(p-2)}{2!}$ different ways. We get a contribution :

$$\frac{(p-1)(p-2)}{2!} (R_{22})^{(p-3)} (D_{12}D_{21})^2 \int_0^{\zeta_p^{\pm}} d\varphi_1 \int_0^{\zeta_p^{\pm} - \varphi_1} d\varphi_2 \int_0^{\zeta_p^{\pm} - \varphi_1 - \varphi_2} d\varphi_3 =$$

$$= \frac{(p-1)(p-2)}{2!} (R_{22})^{(p-3)} (D_{12}D_{21})^2 \frac{(\zeta_p^{\pm})^3}{3!} \tag{17}$$

Taking all the possible contributions into account, the p-th term gives :

$$f_d^{(p)\pm}(\beta, \vartheta) = \frac{i^{n_p^{\pm}}}{(\sin \vartheta)^{1/2}} D_1^2 D_{12}D_{21} e^{2ip\beta\sqrt{N^2-1}} e^{i\lambda_1 \zeta_p^{\pm}} \cdot$$

$$\cdot \sum_{m=1}^{p} \binom{p-1}{m-1} (R_{22})^{(p-m)} (D_{12}D_{21})^{(m-1)} \frac{(\zeta_p^{\pm})^m}{m!} \tag{18}$$

where $n_p^- = n_p^+ - 1$.

At this point, in order to pass from the kinematical description, like that given by the ray tracing, to a dynamical theory, one must do precise statements on the "coupling constants" and on the surface wave "propagators". In virtue of the "localization principle" (see the Introduction), we can conjecture that the grazing rays undergo the same type of "interactions" as in the case of a wholly transparent sphere. More precisely, we make the following assumptions :

a) The total reflection takes place, i. e.

$$R_{22} = 1 . \tag{19}$$

b) The transmission coefficient, like the reflection coefficient, depends merely on the properties of the sphere at the point of refraction and on the angle of incidence ; therefore we assume for the "coupling constants" D_{12} and D_{21} the same values which have been obtained in the case of a wholly transparent sphere[2] and of a wholly transparent cylinder[6], i. e.

$$D_{12}D_{21} = \frac{2}{\sqrt{N^2-1}} . \tag{20}$$

c) The diffraction coefficients D_n and the decay exponents α_n (and therefore the "propagator" constants $\lambda_n = \beta + i\alpha_n$) depend only on the properties of the spherical surface.

This implies that we can assume for these coefficients the same k-dependence as it was calculated for a wholly transparent sphere[2]. Thus we have:

$$D_n^2 = d_n^2 \, \beta^{-1/6} \tag{21}$$

and

$$\mathrm{Re}\, \lambda_n = \beta + a_n \, \beta^{1/3} \tag{22a}$$

$$\mathrm{Im}\, \lambda_n = b_n \, \beta^{1/3} \, . \tag{22b}$$

Note that, in the case of a wholly transparent sphere, the terms λ_n represent the locations, in the complex angular momentum plane, of those poles of the Debye expansion of the S-function, which lie in the first quadrant[2].

In conclusion formula (18) can be rewritten as follows:

$$f_d^{(p)\pm}(\beta, \vartheta) = \frac{d_1^2 \, i^{n_p^\pm}}{\beta^{1/6} (\sin \vartheta)^{1/2}} \, e^{2ip\beta \sqrt{N^2-1}} \, e^{i\lambda_1 \zeta_p^\pm} \sum_{m=1}^{p} \binom{p-1}{m-1} \left(\frac{2\zeta_p^\pm}{\sqrt{N^2-1}} \right)^m \frac{1}{m!} =$$

$$= \frac{d_1^2 \, i^{n_p^\pm}}{\beta^{1/6} (\sin \vartheta)^{1/2}} \, e^{2ip\beta \sqrt{N^2-1}} \, e^{i\lambda_1 \zeta_p^\pm} \, L_p^{(-1)}(-X_\pm^p) \tag{23}$$

where $X_\pm^p = \frac{2\zeta_p^\pm}{\sqrt{N^2-1}}$ and $L_p^{(-1)}$ is a generalized Laguerre polynomial defined in the following way[2]:

$$L_p^{(-1)}(x) = \frac{x e^{-x}}{p!} \frac{d^p}{dx^p} (x^{p-1} e^x) = \sum_{m=1}^{p} \binom{p-1}{m-1} \frac{x^m}{m!} \tag{24}$$

The total diffraction amplitude is given by the sum (4). Should we extend to infinity this sum, the series would diverge. However, as pointed out by Nussenzveig[2], each term (23) represents only the main contribution for a fixed p and β sufficiently large, whereas we are interested in the asymptotic behaviour for fixed β and increasingly large p. Since, for increasing p, the number of neglected terms also increases, for p large enough, (23) no longer represents the dominant term. Nussenzveig[2] has given a heuristic argument to show that the resultant effect, due to the correction terms, brings about an exponential damping factor for large p. Then the remainder of the sum (4) after P terms is negligible, where P is of the order of magnitude of $\beta^{2/3}$. In conclusion we have:

$$f_d(\beta, \vartheta) \sum_0^P p \left\{ f_d^{(p)+}(\beta, \vartheta) + f_d^{(p)-}(\beta, \vartheta) \right\} = \frac{d_1^2}{\beta^{1/6} (\sin \vartheta)^{1/2}} \sum_0^P p \, e^{2ip\beta \sqrt{N^2-1}} \cdot$$

$$\cdot \left\{ i^{n_p^+} L_p^{(-1)}(-X_+^p) \, e^{i\lambda_1 \zeta_p^+} + i^{n_p^-} L_p^{(-1)}(-X_-^p) \, e^{i\lambda_1 \zeta_p^-} \right\} . \tag{25}$$

Let us remark that formula (25) does not hold within certain angular regions. Indeed at forwards and at backwards the diffracted rays from an axial caustic, so that the approximation, which we assumed, fails in a neighborhood of $\vartheta = 0$ and $\vartheta = \pi$. Moreover at the angles $\vartheta = p\vartheta_t$ (p=1, 2, ...)

we must take into account the contributions of the "critically refracted" geometrical rays. Furthermore in neighborhoods of these angles, one cannot neglect exponentials like $e^{i\lambda_n \zeta_p^{\pm}}$ with $n > 1$; indeed, as one can see from fromula (22b), the simplifying assumption (b) is no longer suitable when

$$\left| \vartheta - p\vartheta_t \right| < \beta^{-1/3} \quad . \tag{26}$$

In other words in these angular regions, which will be called "transition regions", all the surface waves contribute.

It is worth illustrating this point in a more detailed way. For $p = 0$ the inequality (26) defines a region which includes the forward diffraction peak. Here the surface waves give rise to a divergent contribution. On the other hand, near $\vartheta = 0$, the incident and reflected rays have nearly the same directions. From this it follows that also the geometrical contribution presents a divergence at forwards, which compensates the divergence of the surface waves[1].

For $\vartheta = \vartheta_t$ the surface waves relative to the term $p = 1$ are excited. Therefore this angle is a transition point between two different regions, since here the surface wave contribution changes abruptly. Moreover we have also the geometrical contribution of the critically refracted rays. In conclusion we can say that a neighborhood of $\vartheta = \vartheta_t$ is a transition region. We have an analogous situation for $\vartheta = p\vartheta_t$ $(p = 2, 3, \ldots)$.

As far as the backward direction is concerned we shall return on this question later on.

Now it is convenient to distinguish between two different angular regions.

A) When $\pi - \vartheta$ is large, the contribution from $f_d^{(p)-}$ is negligible. Therefore formula (25) can be approximated by:

$$f_d(\beta, \vartheta) \simeq \sum_0^P p\, f_d^{(p)+}(\beta, \vartheta) = \frac{d_1^2}{\beta^{1/6} (\sin\vartheta)^{1/2}} \left\{ \sum_0^P p\, e^{2ip\beta\sqrt{N^2-1}}\, i^{n_p^+} \cdot L_p^{(-1)}(-X_+^p)\, e^{i\lambda_1 \eta_p} \right\} e^{i\lambda_1 \vartheta} \tag{27}$$

where $\eta_p = \zeta_p^+ - \vartheta$. Then, neglecting the reflected ray contribution (we shall discuss this approximations in the next Section), we have:

$$\frac{d\sigma}{d\Omega} \simeq R^2 \left| f_d(\beta, \vartheta) \right|^2 = \frac{R^2 \left| d_1 \right|^4}{\beta^{1/3}} \left| F(\beta, N, \vartheta) \right|^2 \frac{e^{-2\mathrm{Im}\,\lambda_1 \vartheta}}{\sin\vartheta} \tag{28}$$

where

$$F(\beta, N, \vartheta) = \sum_0^P p\, e^{2ip\beta\sqrt{N^2-1}}\, i^{n_p^+}\, L_p^{(-1)}(-X_+^p)\, e^{i\lambda_1 \eta_p} \quad . \tag{29}$$

If we suppose to consider an angular domain, which does not include any transition region, then we can assume that $F(\beta, N, \vartheta)$ depends weakly on ϑ (at least in comparison with $\frac{e^{i\lambda_1 \vartheta}}{(\sin\vartheta)^{1/2}}$). Therefore we get, for a fixed value of k:

$$\frac{d\sigma}{d\Omega} \simeq C_o \frac{e^{-2\mathrm{Im}\,\lambda_1 \vartheta}}{\sin\vartheta} \tag{30}$$

where $C_o = \frac{R^2 \left| d_1 \right|^4}{\beta^{1/3}} \left| \bar{F} \right|^2$, and $\bar{F}$ is the mean value of F over the ϑ interval considered.

Finally from (29) it is apparent that the value of C_o changes abruptly crossing a transition region.

B) Now we consider the angular region where $(\pi - \vartheta)$ is small. Then let us rewrite $\zeta_p^{\pm}$ as follows: $\zeta_p^{\pm} = \nu_p \mp (\pi - \vartheta)$, where $\nu_p = \pi - p\,\vartheta_t \pmod{2\pi}$, $(0 \leq \nu_p \leq 2\pi)$. Next, in the generalized Laguerre polynomials, we replace $\zeta_p^{\pm}$ with ν_p, since $(\pi - \vartheta)$ is small, and we write:

$$f_d(\beta,\vartheta) \simeq \frac{d_1^2}{\beta^{1/6}(\sin\vartheta)^{1/2}} \left\{ \sum_0^P p\, e^{2ip\beta\sqrt{N^2-1}}\, L_p^{(-1)}\left(-\frac{2\nu_p}{\sqrt{N^2-1}}\right) e^{i\lambda_1\nu_p} \cdot \left(i^{n_p^+} e^{-i\lambda_1(\pi-\vartheta)} + i^{n_p^-} e^{i\lambda_1(\pi-\vartheta)} \right) \right\} . \tag{31}$$

Since $n_p^- = n_p^+ - 1$, we can rewrite formula (31) as follows:

$$f_d(\beta,\vartheta) \simeq G\beta^{1/3} \left\{ \sum_0^P p\, e^{2ip\beta\sqrt{N^2-1}}\, L_p^{(-1)}\left(-\frac{2\nu_p}{\sqrt{N^2-1}}\right) e^{i\lambda_1\nu_p} i^{n_p^+} \right\} \cdot \left(\frac{e^{(-i\lambda_1(\pi-\vartheta)+i\frac{\pi}{4})} + e^{(i\lambda_1(\pi-\vartheta)-i\frac{\pi}{4})}}{(2\pi\beta\sin\vartheta)^{1/2}} \right) \tag{32}$$

where $G = (2\pi)^{1/2}(d_1)^2 e^{-i\pi/4}$. But the last factor in formula (32) is simply the asymptotic behaviour of $P_{\lambda_1 - \frac{1}{2}}(-\cos\vartheta)$ (i.e. the Legendre function of the first kind with index $\lambda_1 - \frac{1}{2}$), when $|\lambda_1| \to \infty$, $|\lambda_1|(\pi - \vartheta) \gg 1$ and λ_1 is approximated by β in the denominator. Furthermore we assume that at backwards the sum (4) is dominated by the term which corresponds to the shortest path of the surface waves, say $p = \bar{p}$. In conclusion we write:

$$f_d(\beta,\vartheta) \simeq G\beta^{1/3} \left\{ e^{2i\bar{p}\beta\sqrt{N^2-1}}\, L_{\bar{p}}^{(-1)}\left(-\frac{2\nu_{\bar{p}}}{\sqrt{N^2-1}}\right) e^{i\lambda_1\nu_{\bar{p}}} i^{n_{\bar{p}}^+} \right\} P_{\lambda_1 - \frac{1}{2}}(-\cos\vartheta) \tag{33}$$

where we use explicitly the Legendre function $P_{\lambda_1 - \frac{1}{2}}(-\cos\vartheta)$ instead of its asymptotic behaviour. This function is regular for $\vartheta = \pi$, and we can assume that formula (33) holds true even in a neighbourhood of the angle $\vartheta = \pi$. Finally, neglecting the reflected ray contribution, we have:

$$\frac{d\sigma}{d\Omega} = R^2 \left| f_d(\beta,\vartheta) \right|^2 \simeq A_o \beta^{2/3} e^{-2\mathrm{Im}\,\lambda_1\nu_{\bar{p}}} \left| P_{\lambda_1 - \frac{1}{2}}(-\cos\vartheta) \right|^2 \tag{34}$$

where

$$A_o = R^2 |G|^2 \left| L_{\bar{p}}^{(-1)}\left(-\frac{2\nu_{\bar{p}}}{\sqrt{N^2-1}}\right) \right|^2 .$$

In order to fit the experimental data, it is convenient to express the differential cross section as a function of the Lorentz invariant variables t and u (Mandelstam variables). Then, in place of formula (30), we have:

$$\frac{d\sigma}{d|t|} \simeq C\, \frac{e^{-2\mathrm{Im}\,\lambda_1\vartheta}}{\sin\vartheta} , \qquad C = \frac{\pi C_o}{K^2} . \tag{35}$$

At backwards we have:

$$\frac{d\sigma}{du} = A \left| P_{\lambda_1 - \frac{1}{2}}(-\cos\vartheta) \right|^2 \tag{36}$$

where

$$A = \pi K^{-2} A_o \beta^{2/3} e^{-2 \mathrm{Im}\lambda_1 \nu_{\bar{p}}} . \tag{37}$$

Substituting formula (22b) into (37) we obtain:

$$A = A_1 K^{-4/3} e^{-cK^{1/3}} \tag{38}$$

with

$$A_1 = \pi A_o R^{2/3} \qquad \text{and} \qquad c = 2 b_1 \nu_{\bar{p}} .$$

Lastly, since $P_{\lambda_1 - \frac{1}{2}}(-\cos\vartheta) = 1$ for $\vartheta = \pi$, from (36) we have:

$$\left(\frac{d\sigma}{du}\right)_{\vartheta=\pi} = A = A_1 K^{-4/3} e^{-cK^{1/3}} . \tag{39}$$

3. - PHENOMENOLOGICAL ANALYSIS.

In a previous paper[7] (which will be referred hereafter as I) the backward differential cross section of the elastic scattering of pions from an unpolarized proton target, in the momentum range 3.55 - 7.00 GeV/c, has been fitted with the following formula(x):

$$\frac{d\sigma}{du} \simeq A \left| P_{\lambda_1 - \frac{1}{2}}(-\cos\vartheta) \right|^2 + B \left| P^1_{\lambda_1 - \frac{1}{2}}(-\cos\vartheta) \right|^2 \tag{40}$$

where $P^1_{\lambda_1 - \frac{1}{2}}$ is an associated Legendre function, which has been introduced in order to take into account the spin of the proton (indeed the second term of (40) corresponds to the spin-flip amplitude). If $B = 0$ formula (40) reduces to formula (36). In I we obtained, with formula (40), very accurate fits, at fixed energy, in the angular region: $0.80 < -\cos\vartheta_{c.m.} < 1$ (see Figs. 1 2, 3 of I). By these fits we derived the values of $\mathrm{Re}\,\lambda_1$ and $\mathrm{Im}\,\lambda_1$ at three different energies, and so it was possible to draw phenomenological trajectories of $\mathrm{Re}\,\lambda_1$ and $\mathrm{Im}\,\lambda_1$ versus s (= squared energy in the centre of mass system); see Figs. 4 and 5 of I. However, the second of these trajectories does not show any precise law in the dependence of $\mathrm{Im}\,\lambda_1$ on s. In this connection let us remark that there was some arbitrariness in choosing the angular region where we tried to fit the data. In order to make possible the comparison of the values of $\mathrm{Re}\,\lambda_1$ and $\mathrm{Im}\,\lambda_1$ at different energies, it seems more appropriate to keep the range of the variable u fixed, rather than $\cos\vartheta_{c.m.}$, compatibly with the available experimental data. Indeed both the minima and the following maxima in the differential cross-sections occur at the same u-values[8]. For this reason we report here the fit of the data at $p_{Lab} = 3.55$ GeV/c (see Fig. 3), since in I the range of the variable u for this set of data was somewhat different from the other ones. Furthermore, in order to complete our phenomenological analysis, we report here two other fits (the experimental data used, as well as those fitted in Fig. 3, are given in refs. (8, 9)), performed with formula (40); they are given in Figs. 4 and 5.

(x) - In I we have written α in the place of $\lambda_1 - \frac{1}{2}$.

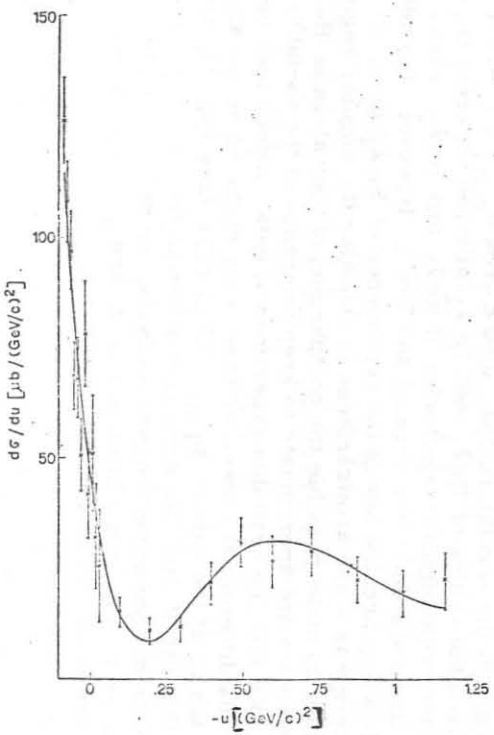

FIG. 3 - Differential cross section $d\sigma/du$, at $p_{Lab} = 3.55$ GeV/c;
$-1.175\,(GeV/c)^2 < u < 0.083\,(GeV/c)^2$.
The fit parameters are:
$A = 131.9\ \mu b/(GeV/c)^2$,
$B = 0.45\ \mu b/(GeV/c)^2$,
$Re\,\lambda_1 = 5.47$, $Im\,\lambda_1 = 0.76$.
The χ^2 value is 15.1 and the χ^2 test gives a probability of ~60%.

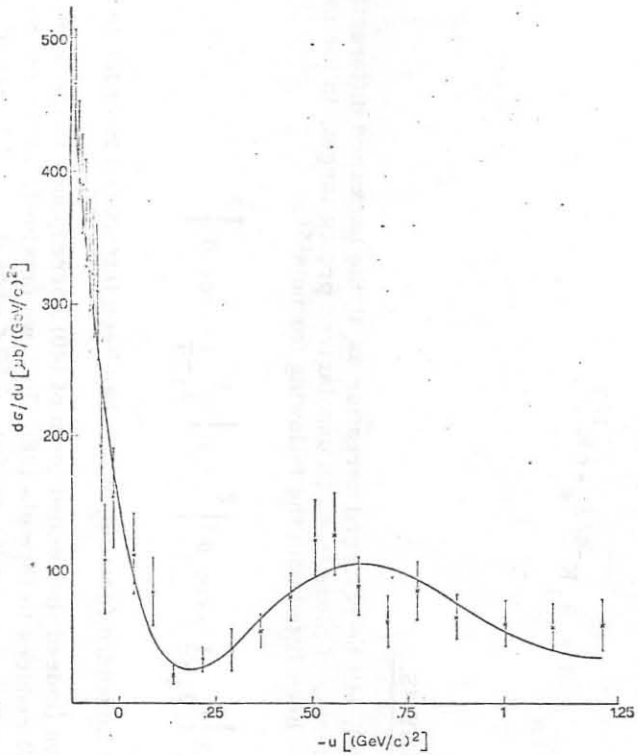

FIG. 4 - Differential cross section $d\sigma/du$, at $p_{Lab} = 2.85$ GeV/c;
$-1.238\,(GeV/c)^2 < u < 0.107\,(GeV/c)^2$.
The fit parameters are:
$A = 494.6\ \mu b/(GeV/c)^2$,
$B = 2.78\ \mu b/(GeV/c)^2$,
$Re\,\lambda_1 = 4.72$, $Im\,\lambda_1 = 0.45$.
The χ^2 value is 26.5 and the χ^2 test gives a probability of ~35%

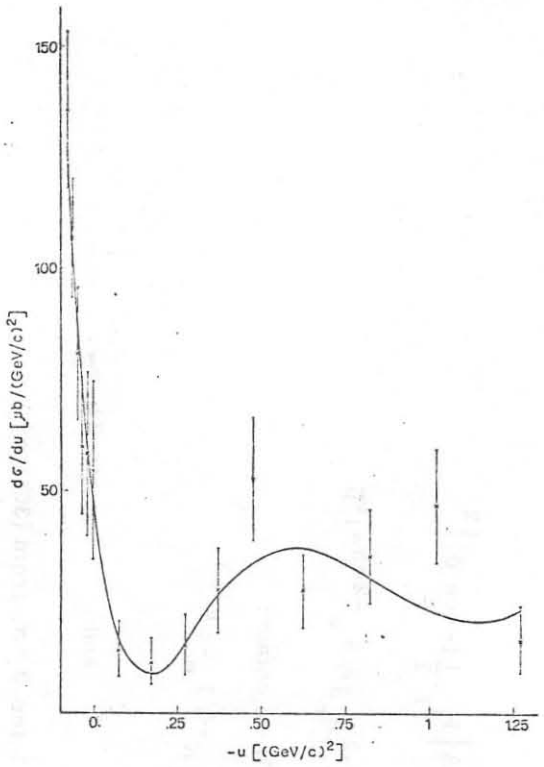

FIG. 5 - Differential cross section $d\sigma/du$, at $p_{Lab} = 3.30$ GeV/c;
$-1.275\,(GeV/c)^2 < u < 0.088\,(GeV/c)^2$.
The fit parameters are:
$A = 145.1\ \mu b/(GeV/c)^2$,
$B = 0.22\ \mu b/(GeV/c)^2$,
$Re\,\lambda_1 = 5.35$, $Im\,\lambda_1 = 0.86$.
The χ^2 value is 9.45 and the χ^2 test gives a probability of ~60%.

Then, using formula (22a, b) we can fit Re λ_1 and Im λ_1 versus $p_{c.m.} = \hbar K$ (recall that the values of Re λ_1 and Im λ_1 at $p_{Lab} = 5.20$ GeV/c and $p_{Lab} = 7.00$ GeV/c are those obtained in I). The fit of Re λ_1 versus $p_{c.m.}$ will be discussed later on (see Fig. 12). The fit of Im λ_1 versus $p_{c.m.}$ is reported in Figs. 6a and 6b. Fig. 6a shows that the agreement between the data and the

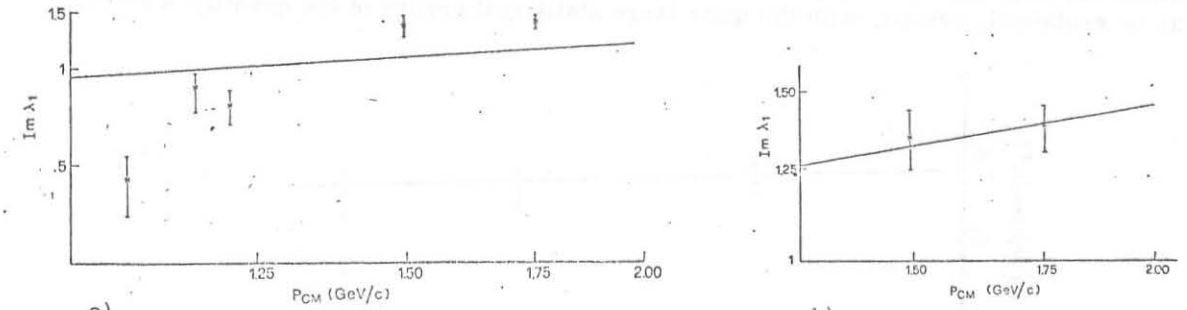

FIG. 6 - Im λ_1 versus $p_{c.m.} = \hbar K$. a) All the available data are considered; the fit parameter (see formula (22b)) is: $b_1 R^{1/3} = 0.55$ (fm)$^{1/3}$. b) Only the data at $p_{Lab} = 5.2$ GeV/c and 7.0 GeV/c are considered; the fit parameter is: $b_1 R^{1/3} = 0.67$ (fm)$^{1/3}$; the χ^2 value is 0.05 and the χ^2 test gives a probability of $\sim$80%.

fitting curve is not satisfactory. But it becomes very good if we fit only the two data at higher momenta (see Fig. 6b). This fact can be tentatively explained as follows:

a) Our model does work only if $\beta \gg 1$; this condition is not yet satisfied at lower momenta. Indeed the data at lower momenta are quite near to the resonance region.

b) The values of Im λ_1, considered in Fig. 6a, have been derived by fitting data sets obtained in different experiments. Indeed the three points at lower momenta derive from one experiment[10]; the two points at larger momenta (considered in Fig. 6b) derive from another one[8, 9]. The discrepancy might be due, perhaps, to different normalizations in the experiments.

Finally let us observe that, in the energy interval analyzed, the effect of the spin is negligible, i.e. $B \simeq 0$. Therefore, hereafter, we shall discard the effect of the spin, as we said before.

Next we try a fit at fixed angle, i.e. $\vartheta_{c.m.} = \pi$, with formula (39). Indeed we have experimental data in the momentum range 3.3-6.00 GeV/c[11]. The fit is reported in Fig. 7. Let us observe that the theoretical curve does not reproduce some small oscillations that the experimental data exhibit. These could be due to the interference of the principal term, $p = \bar{p}$, with one or more terms, which we have neglected in the sum (32).

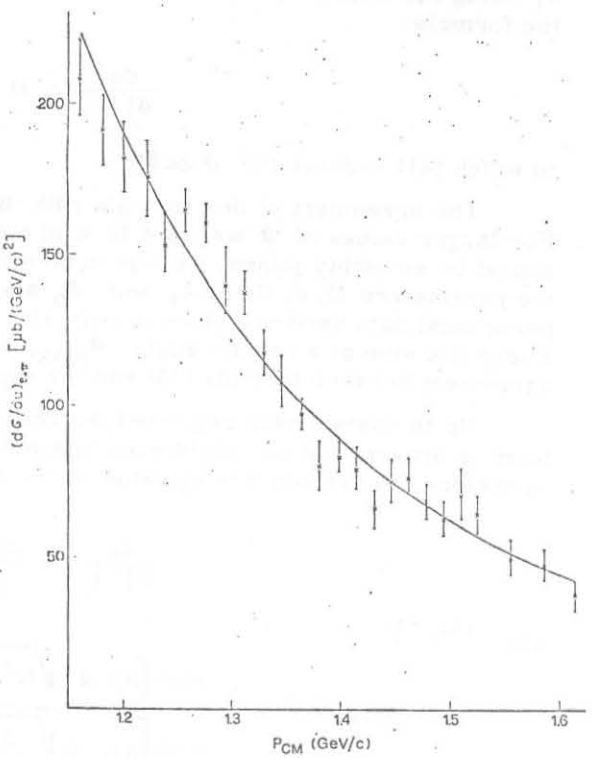

FIG. 7 - The differential cross section $(d\sigma/du)_{\vartheta_{c.m.}=\pi}$ versus $p_{c.m.}$. The fit parameters are:
$A_1 = 9.92 \times 10^6$ μb/(GeV/c)$^{2/3}$,
$c = 5.82$ (fm)$^{1/3}$.

At this point we have determined the parameter c (which appears in formula (39)), by means of the preceding fit at $\vartheta_{c.m.} = \pi$. Moreover we know also the values of A (see formula (36)) at different values of K. Then we can test whether the quantity $A\, e^{cK^{1/3}}$ is proportional to $K^{-4/3}$, as prescribed by formula (38). The fit is reported in Fig. 8. In this case we have an agreement between the data and the fitting curve which does not require any subdivision of the data. This fact may be explained, pehaps, with the quite large statistical errors of the quantity $A\, e^{cK^{1/3}}$.

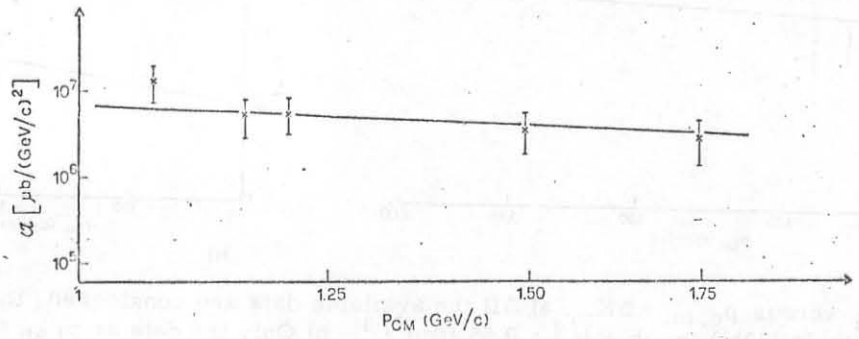

FIG. 8 - The quantity $\alpha = A\, e^{cK^{1/3}}$ versus $p_{c.m.}$. The fit parameter is : $A_1 = 6.89 \times 10^6\ \mu b/(GeV/c)^{2/3}$.

As we said in Section 2, at forward we have the diffraction peak. In our model the diffraction peak is described by the following formula[1,2], which holds true for $\vartheta \ll \beta^{-1/3}$

$$\frac{d\sigma}{d|t|} \propto \left(\frac{J_1(\beta\vartheta)}{\beta\vartheta} \right)^2 \tag{41}$$

J_1 being the Bessel function of index 1. Phenomenologically the data suggest that we should use the formula :

$$\frac{d\sigma}{d|t|} = D\, e^{-b|t|} \tag{42}$$

to which (41) reduces for $\vartheta \ll \beta^{-1}$.

The agreement of this formula with the data ceases to exist at a certain angle, say ϑ_o. For larger values of ϑ we try a fit with the use of formula (35). Now the functions (42) and (35) should be smoothly joined ; we link them simply imposing the continuity at $\vartheta = \vartheta_o$. Therefore the parameters D, b, C, $\mathrm{Im}\,\lambda_1$ and ϑ_o are not all independent. We fit three sets of data (the experimental data used are given in refs. (12, 13)). The results are presented in Figs. 9, 10 and 11. These fits stop at a certain angle ϑ_{Max}, where the cross section rises again and therefore the agreement between formula (35) and the experimental data is no longer satisfactory.

Up to now we have neglected the reflected ray contribution for $\vartheta > \vartheta_o$. Of course this term is present and one could even argue that it is dominant, at least at not too large angles. Therefore, to exclude this hypothesis, we have tried a fit with the following formula (for $\vartheta > \vartheta_o$):

$$\frac{d\sigma}{d|t|} = \frac{\pi R^2}{K^2} \left| f_r(\beta, \vartheta) \right|^2 \tag{43}$$

where[14, 15]

$$f_r(\beta, \vartheta) = -\frac{1}{2} \frac{\sinh\left[\pi K \Delta \left(\sqrt{N^2 - \cos^2\frac{\vartheta}{2}} - \sin\frac{\vartheta}{2} \right)\right]}{\sinh\left[\pi K \Delta \left(\sqrt{N^2 - \cos^2\frac{\vartheta}{2}} + \sin\frac{\vartheta}{2} \right)\right]} e^{-2i\beta \sin\frac{\vartheta}{2}} \tag{44}$$

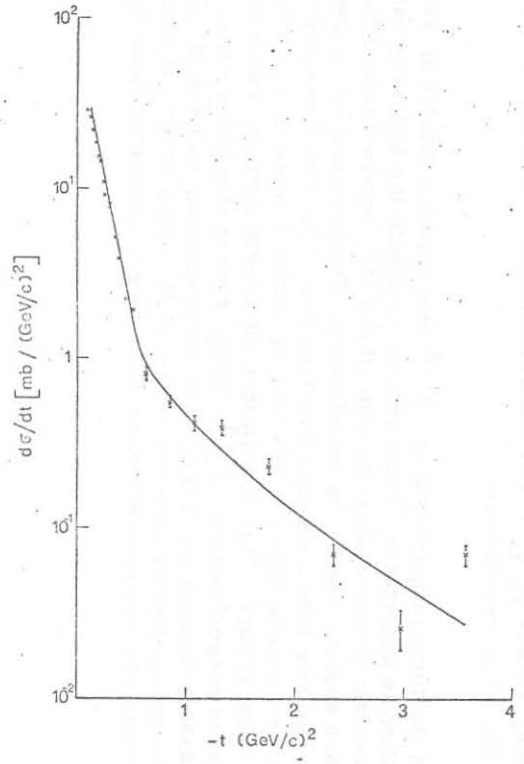

FIG. 9 - Differential cross section $d\sigma/d|t|$ at p_{Lab} = 3.0 GeV/c, 0.085 (GeV/c)^2 < -t < 3.58 (GeV/c)^2. The fit parameters are: D = 54.1 mb/(GeV/c)^2, b = 16.5 (GeV/c)$^{-2}$, C = 3.66 mb/(GeV/c)^2, Im λ_1 = 1.21, ϑ_o = 0.71 rad. The χ^2 value is 61.1.

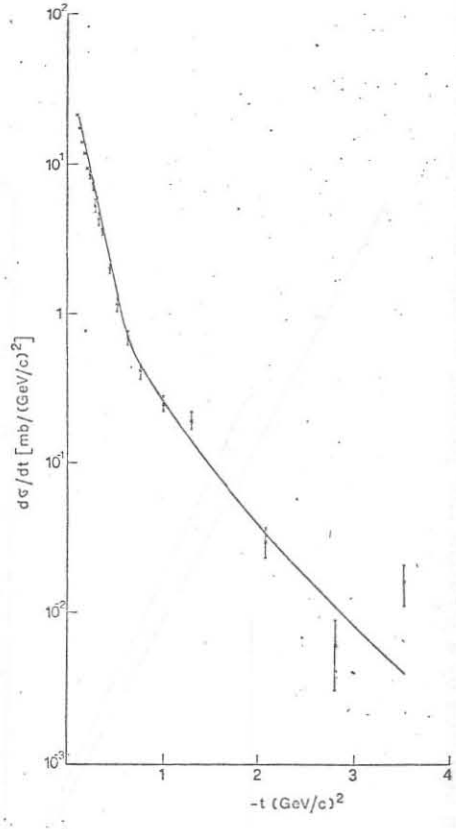

FIG. 10 - Differential cross section $d\sigma/d|t|$ at p_{Lab} = 3.50 GeV/c, 1.01 (GeV/c)^2 < -t < 4.26 (GeV/c)^2. The fit parameters are: D = 41.5 mb/(GeV/c)^2, b = 19.3 (GeV/c)$^{-2}$, C = 7.07 mb/(GeV/c)^2, Im λ_1 = 2.07, ϑ_o = 0.65 rad. The χ^2 value is 28.7

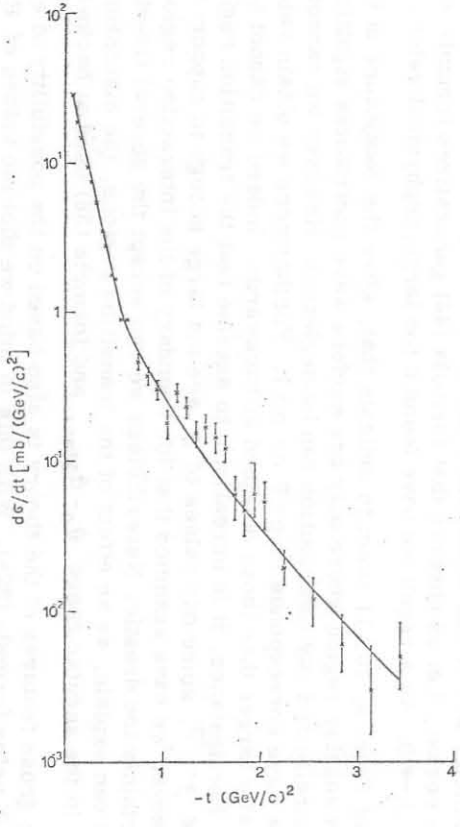

FIG. 11 - Differential cross section $d\sigma/d|t|$ at p_{Lab} = 3.63 GeV/c, 0.075 (GeV/c)^2 < -t < 3.45 (GeV/c)^2. The fit parameters are: D = 44.3 mb/(GeV/c)^2, b = 19.8 (GeV/c)$^{-2}$, C = 11.4 mb/(GeV/c)^2, Im λ_1 = 2.36, ϑ_o = 0.63 rad. The χ^2 value is 42.8.

Δ being the diffuseness parameter and N the maximum value of the real part of the "refraction index" inside the interaction region. Let us observe that formula (44) generalizes formula (3); indeed it reduces to (3) for $\Delta \rightarrow 0$. As a result we have found a too large, unphysical value of R.

In conclusion the fits of Figs. 9, 10, 11 seem to indicate that, after the dominance of the diffractive peak, there is an angular region where only one surface wave contributes significantly and its interference with the reflected ray contribution can be neglected. However we cannot say, at the moment, whether this wave corresponds to $p = 0$ or $p = 1$. Furthermore we obtain values of $\mathrm{Im}\,\lambda_1$ which are systematically larger than those obtained at backwards. Indeed we cannot believe in the details of the model. For instance, it is unrealistic to assume that the transition regions for $p \gtrsim 1$ are of the order of $\beta^{-1/3}$, since our values of β are not large enough to support fully an asymptotic theory. Moreover we have assumed that the boundary of the interaction region has a sharpe edge, which is certainly too drastic. Nevertheless we can accept the general trends of the model. In particular we can explain, as an effect of the transition regions, the discontinuity between formula (35), used in the angular range $\vartheta_o - \vartheta_{Max}$, and formula (36) used at backwards.

Our confidence on the gross features of the theory is also based on the possibility of evaluating the interaction radius R using formula (22a). With this in mind we plot the values of $\mathrm{Re}\,\lambda_1$ versus $p_{c.m.}$ (recall that these values have been obtained by the fits at backwards) and observe that these five points can be subdivided into two groups. The first group is composed of the two data at larger momenta; in the second one there remain three points at lower momenta (recall that we have done an analogous subdivision in connection with the fits reported in Figs. 6a, b). The data of the first set can be fitted by a straight line passing through the origin (see Fig. 12).

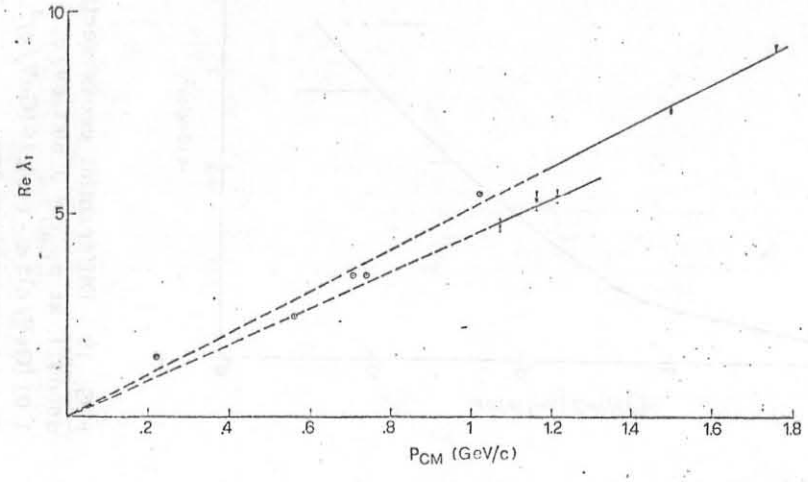

FIG. 12 - $\mathrm{Re}\,\lambda_1$ versus $p_{c.m.}$. The encircled points denote the locations of the π^+-p resonances.

So doing we have neglected the term proportional to $\beta^{1/3}$ (see formula (22a)); as we shall see in a moment, this approximation is acceptable. From this fit we obtain the following value for R: 1.017 ± 0.006 fm. The agreement of this evaluation with others[16], obtained with different models and using data in the forward angular region, is satisfactory. Furthermore let us observe that the π^+-p resonances lie along this fitting straight line (see Fig. 12). The three points at lower momenta can also be fitted by formula (22a); in this way we obtain a value of a_1, which turns out to be zero within the statistical errors. This legitimates the approximation, which has been done before, of neglecting the term proportional to $\beta^{1/3}$. Then, also in this latter case, we fit the data with a straight line passing through the origin. The corresponding value of R is: $0.882 \pm \pm 0.014$ fm. The small discrepancy between the two values of R, which have been obtained, can probably be explained recalling the remarks which we have done in connection with the fits of Figs. 6a, b.

ACKNOWLEDGEMENTS.

It is a pleasure to thank our friends Profs. R. Anni, A. Santroni and U. Trevisan for many suggestions and enlightening discussions.

REFERENCES.

(1) - B. Schrempp and F. Schrempp, Lett. Nuovo Cimento 20, 95 (1978); Phys. Letters 70B, 88 (1978).
(2) - H. M. Nussenzveig, Jnl. Math. Phys. 10, 82 (1969); 10, 125 (1969).
(3) - J. B. Keller, Proc. Symp. Applied Mathematics 8, 27 (1958).
(4) - B. R. Levy and J. B. Keller, Comm. Pure Appl. Math. 12, 159 (1959).
(5) - R. Anni and L. Taffara, Nuovo Cimento 31A, 321 (1976).
(6) - Y. M. Chen, Jnl. Math. Phys. 5, 820 (1964).
(7) - E. Di Salvo and G. A. Viano, Nuovo Cimento 42A, 49 (1977).
(8) - J. Banaigs, J. Berger, C. Barnel, J. Duflo, L. Goldzahl, F. Plouin, W. F. Baker, P. J. Carlson, V. Chabaud and A. Lundby, Nuclear Phys. 8B, 31 (1968).
(9) - W. F. Baker, P. J. Carlson, V. Chabaud, A. Lundby, J. Banaigs, J. Berger, C. Bonnel, J. Duflo, L. Goldzahl and F. Plouin, Nuclear Phys. 9B, 249 (1969).
(10) - W. F. Baker, K. Berkelman, P. J. Carlson, G. P. Fisher, P. Fleury, D. Hartill, R. Kalbach, A. Lundby, S. Mukhin, R. Nierhaus, K. P. Pretzland and J. Woulds, Nuclear Phys. 25B, 385 (1971).
(11) - A. J. Lennox, J. A. Poirier, C. A. Rey, O. R. Sander, W. F. Baker, D. P. Eartly, K. P. Pretzl, S. M. Prussand and A. A. Wehmann, Phys. Rev. 11D, 1777 (1975).
(12) - C. T. Coffin, N. Dirkmen, L. Ettlinger, D. Meyer, A. Saulys, K. Terwilliger and D. Williams, Phys. Rev. 159, 1169 (1967).
(13) - J. Mac Naughton, W. R. Butler, D. G. Cayne, G. M. Hicks and G. H. Trilling, Nuclear Phys. 33B, 101 (1971).
(14) - L. Landau and E. Lifchitz, Mecanique Quantique (Moscow, 1966), p. 100.
(15) - R. Anni, L. Renna and L. Taffara, Nuovo Cimento 45A, 122 (1978).
(16) - G. Giacomelli, Riv. Nuovo Cimento 2, 297 (1970).